Available online www.jsaer.com

***Journal of Scientific and Engineering Research*, 2016, 3(3):574-589**

Research Article

ISSN: 2394-2630
CODEN(USA): JSERBR

Micro-Kinetics Evaluation of Coag-flocculation Factors for *Telfairia Occidentali's* Seed Biomass in Pharmaceutical Effluent System

Ugonabo VI, Menkiti MC, Onukwuli OD

Department of Chemical Engineering, Nnamdi Azikiwe University,Awka, Nigeria.

Abstract Micro-kinetics evaluation of coag-flocculation factors for *Telfairia occidentalis* seed biomass in pharmaceutical industry effluent (PIE) system has been investigated at room temperature, following standard method of bench scale jar test. *Telfairia occidentalis* seed biomass (TOSC) was prepared according to work reported by Ugonabo, *et al.*, 2012. The data obtained were fitted into specified kinetic model for the evaluation of functional parameters. The optimal values of pH, dosage and settling time were recorded at 13, $0.1x10^{-3}kg/m^3$and 2400secs respectively. The result of the major functional parameters, obtained are 2,7.5 E – $05m^3/kg.s$, and 12.68secs for order of reaction, coag-flocculation rate constant and coagulation period, respectively. At optimum, the total dissolved and suspended solids (TDSS) was reduced from 2070 mg/l to 211.97mg/l, representing 89.76% removal efficiency. Comparatively, *Telfairia occidentalis* seed biomass has reaffirmed its effectiveness even at the pH domain of alum as an alternative resource for water purification at the prevailing condition of the experiment.

Keywords Coag-flocculation, pharmaceutical effluent, *Telfairia occidentalis* seed biomass.

1. Introduction

Pharmaceutical industry effluents are one of the major causes of environmental pollution and effluents from many other industries which use dyes and pigments [1-2]. The effluents from such industries are characteristically turbid as a result of presence of large amounts of both total dissolved and suspended solid particles inherent [3]. Untreated discharge of this turbid water – notorious pollutant into the environment will be deleterious to the aquifers of pharmaceutical bearing communities in Nigeria. The characteristics of pharmaceutical industry effluent (PIE) is a major determination for employing the most suitable technique and remediation options available for the effluent treatment [4-6]. Depending on the process route, the quality and characteristics of PIE fluctuates significantly [7]. Results show that organic compounds detected in PIE, include; antibiotics, other prescription drugs, non-prescription drugs, animal and plant steroids, analgesics, lipid regulating drugs, antiseptics, hormone, and chemotherapy and beta-blocking heart drugs [8-12]. Typically, untreated PIE contains suspended solids (300 – 400 mg/l), biochemical oxygen demand (1200 – 1700 mg/l), Phenols (65 – 72 mg/l), chemical, Oxygen demand (2,000 – 3,000 mg/l), and dissolved solids (1200 – 1600 mg/l) [1,13] .

There are many processes available for wastewater treatment in industries. Physicochemical, chemical and biological methods, adsorption, electrolysis etc; [14-18]. Among these methods, physicochemical processes has been proved to be effective in the purification of pharmaceutical industry effluent no matter the time lag [19-20]. Coag-flocculation is a commonly applied, simple physicochemical technique widely used for water and wastewater treatment. The removal mechanisms mainly are charge neutralization which connotes other intermediate mechanisms such as double layer compression, sweep flocculation and bridge-aggregation [21-23]. Charge neutralization by double layer compression is accomplished when flocculation is effective via an increase in solution ionic strength. This compression allows the approach of the colloidal particles, where short-range attractive forces predominates over electrostatic repulsive forces. For instance, the presence of hydrolysable metal ions such as Al^{3+} and Fe^{3+} or polyelectrolytes of opposite charge to colloid surface, the charge is neutralized by adsorption of these species onto the particle surface, leading to the flocculation of anionic colloidal particles with cationic polymers. The action of cationic polymers is facilitated by the reduction

of double layer repulsion, resulting in strong attachment on anionic particles, allowing particles aggregation into visible flocs that settles out under gravity for onward removal from the system [24-25].
Inorganic coagulants such as lime and salts of iron, magnesium and aluminum have been used over many years. Among these inorganic coagulants, alum is most commonly used, having optimum turbidity reductions within the pH range 6.0 – 7.5 [26-27] and turbidity removal efficiency from PIE of 93.26% [28]. Though the effectiveness of alum in water purification is established, but several problems has been associated with its usage. There is increase in volume of sludge and also resulting in poor settling and dewatering characteristics. In addition, alum salts used as coagulant aid consumes alkalinity and can depress the pH of the effluent water. Finally, it is most effective over a limited pH range as earlier mentioned. To overcome these problems Telfairia occidentals seed – a natural coagulant is used in a comparative basis with alum to ascertain its effectiveness in PIE treatment.
Telfairia occidentalis is a pod herbs of family cucurbitaceae. It is found in abundance in southern part of Nigeria. Though the present author has done work in this regard, but the removal efficiency and in comparism with alum was not considered. Against this end, this work intend to deal with kinetic functional parameter and performance evaluation of TOSC and alum at varying pH of PIE effluent, TOSC and Alum dosages and settling time. Also, this work compares the role of alternative natural coagulant (TOSC) in its enhancement for turbidity removal with the aluminum-binding properties of commercially available inorganic coagulant. Above all, the optimum conditions for the coag-flocculation activities of TOSC and alum respectively will be ascertained.

2. Kinetic Model Development

For homogenously, interacting coag-flocculation system where Brownian stochastic force dominates; the heating/stirring of the system produces temperature gradient which causes migration of the particles driven by thermally excited gradients of surface tension [29-31] .

$$\nabla_s^{\sigma} = -\frac{E_T \nabla_s^T}{T} \qquad (2.1)$$

Where $E_T = -\frac{\partial \sigma}{\partial \ln T}$

∇_S is the surface gradient operator; σ is the surface tension and E_T is the coefficient of interfacial thermal elasticity. The effect is that particles moving randomly with different velocity can coag-flocculate to form larger flocs.

Assuming mono-disperse, perfect elasticity and bi-particle collisions, the general mode for micro-kinetic coag-flocculation is given as [32] .

$$\frac{dn_k}{dt}_{i=1} = \frac{1}{2} \sum_{i=1}^{k-i} a_{cf}^{i,k-i}\, n_i\, n_{k-i}\, q_k - n_k \sum_{i=1}^{\infty} a_{cf}^{k,i}\, n_{i+}\, q_k \qquad (2.2)$$

(k = 1,2,3)

$\frac{dn_k}{dt}$ is the rate of change of concentration of particle of size, K
Where t is time, n_1 denotes number of mono-particles per unit volume;
n_k is number of the flocs of K aggregates (k = 2,3,4…..) per unit volume; a_{cf} (i,j = 1,2,3….) is a function of coag flocculation transport mechanism; q_k denotes flux of flocs of size k.
In case of irreversible coagulation q_k = 0. The total concentration of flocs, N and total concentration of the constituent particles (including those in flocculated form) N_t, are given by the expressions

$N = \Sigma n_k$, $N_t = \Sigma K n_k$ (2.3)

Also $a_{cf} = 4\pi D^o$ i,j $(R_i + R_j)$ Ei, j (2.4)

Similarly, for Brownian transport is given as [32] .

$$(a_{cf})_{BR} = \frac{8}{3} \varepsilon_p \frac{k_B T}{\eta} \qquad (2.5)$$

Where $D^{(0)}_{i,j}$ is the relative diffusion coefficients for two flocs of radii R_i and R_j, and aggregation number i and j, respectively; $E_{i,j}$ is the collision efficiency [33] ; [34]; $\varepsilon_p = E_{i,j}$ -collision efficiency.The aggregation rate of intending potential particles during coag-flocculation can be obtained by the combination of equations 2.2 and 2.5 yields

$$-\frac{dN_t}{dt} = K N_t^{\alpha} \qquad (2.6)$$

where N_t is the total concentration of constituent particles at time t as expressed in equation 2.3 above
K is the coag-flocculation constant
α is the order of coag-flocculation process.

Equally, $(a_{cf})_{BR} = \varepsilon_p K_f N_t^{\alpha}$ (2.7)

Where K_f is rate constant of flocculation for rapid flocculation. However, for second order (n_o^2) reaction rate constant (K_f)

$$K_f = 8\pi R_o D^1 \quad (2.8)$$

Where R_o is particle radius

D^1 is diffusion coefficient for intending flocculating particles i and j

$$R_p = R_i + R_j \quad (2.9)$$

Where R_p is relative particle radius for R_i and R_j

Putting $R_i = R_o$ and $R_j = R_o$

Equation 2.9 transposes to $R_p = 2R_o$ (2.10)

From Einstein's approach to the theory of diffusivity D^1.

$$D^1 = \frac{k_B T}{B} \quad (2.11)$$

And from stokes equation $B = \frac{F}{V}$ (2.12)

Where K_B – is Boltzman's constant (J/K)

T – is absolute temperature (K)

B – is the friction factor

V – is the velocity acquired by potential aggregating particles under the influence of stochastic force (as result of heat and stirring of the system).

But for a solid sphere of radius R_o, the stokes equation gives

$$B = 6\pi\eta R_o \quad (2.13)$$

where, η - is the viscosity of the coag-flocculating fluid.

Substituting equation 2.11, 2.13 into 2.8 yields

$$K_f = \frac{4}{3}\frac{k_B T}{\eta} \quad (2.14)$$

Combining equations 2.7 to 2.14 gives:

$$K = \frac{1}{2}(a_{cf})_{BR} \quad (2.15)$$

Similarly, $2k = (a_{cf})_{BR} = \varepsilon_p k_f$ (2.16)

Substituting equations 2.5 and 2.15 into 2.6 yields

$$-\frac{dN_t}{dt} = \frac{4}{3}\varepsilon_p \frac{k_B T}{\eta} N_t^{\alpha} \quad (2.17)$$

For micro-kinetic aggregation, α theoretically equals 2 as given [20] .

From Ficks first law; number of particles entering sphere with radius R_P per unit time J_t.

$$J_t = 4\pi R_p^2 D^1 \frac{dN_t}{dR_p} \quad (2.18)$$

where J_t is flux (number of particles per unit surface and unit, time at position R_P integrating equation (2.17) at initial conditions $N_t = 0$, $R_p = 2R_o$.

$$\frac{J_t}{4\pi}\frac{dR_p}{R_p^2}\int_o^{R_p} dR_p = \int_{N_o}^{N_t} d N_t \quad (2.19)$$

Thus $J_t = 8\pi D^1 R_o N_o$ (2.20)

Generally, for particle of same size under the influence of Brownian motion. The initial rate of coag-flocculation is

$$-\frac{dN_t}{dt} = J_t \varepsilon_p N_o \quad (2.21)$$

Substituting equations (2.12), (2.13) and (2.20) into (2.21) yields

$$-\frac{dN_t}{dt} = \frac{4}{3}\varepsilon_p \frac{k_B T}{\eta} N_o^2 \quad (2.22)$$

Similarly

$$-\frac{dN_t}{dt} = \frac{4}{3}\varepsilon_p \frac{k_B T}{\eta} N_t^2 \quad \text{at } t > o$$

Hence, from equation (2.21) putting, α = 2; equation (2.6) transposed to

$$-\frac{dN_t}{dt} = -K N_t^{\alpha} \quad (2.23)$$

Integrating

$$\int_{N_o}^{N_t}\frac{dN_t}{N_t} = -K\int_0^t dt \quad (2.24)$$

Thus $\frac{1}{N_t} = Kt + \frac{1}{N_o}$ (2.25)

Plot of $\frac{1}{N}$ vs t gives a slope of K and intercept of $\frac{1}{N_o}$

On evaluation of equation 2.25, $\tau_{1/2}$ (Coagulation period) can be determined.

$$N_t = \left(\frac{N_o}{1 + \left(\frac{t}{\frac{1}{N_{ok}}} \right)} \right) \quad (2.26)$$

Where $\tau = \left(\frac{1}{N_{ok}} \right)$ (2.27)

Substituting equation (2.27) into (2.26) yields

$N_t = \frac{N_o}{\left(1 + \frac{t}{\tau} \right)}$ (2.28)

As t = τ equation (2.27) transpose to;

$N_t = \frac{N_o}{2}$ (2.29)

Similarly

$N_t = 0.5N_o$

As $N_o \rightarrow 0.5\ N_o$; $\tau \rightarrow \frac{\tau}{2}$,

Hence equation (2.26) becomes

$\frac{\tau}{2} = (0.5\ N_{oK})^{-1}$ (2.30)

For a coagulation period, where total number of concentration N_t is halves, solving equation (2.2) results in the general expression for particle of mth order.

$$\frac{N_m(t)}{N_o} = \frac{[\frac{KN_o t}{2}]^{m-1}}{[1 + \frac{KN_o t}{2}]^{m+1}} \quad (2.31)$$

Recall; $\frac{\tau}{2} = \frac{N_{oK}}{2}$ or $(0.5N_{oK})^{-1}$

For single particle (m = 1)

$$\frac{N_1 t}{N_o} = \frac{1}{\left(1 + \left[\frac{KN_o t}{2} \right] \right)^2} \quad (2.32)$$

$$\therefore N_1 t = \frac{N_o}{\left(1 + \left[\frac{KN_o t}{2} \right] \right)^2} \quad (2.33)$$

For double particles (m = 2)

$$\frac{N_2 t}{N_o} = \frac{[\frac{KN_o t}{2}]^2}{\left(1 + \frac{KN_o t}{2} \right)^3} \quad (2.34)$$

$$\therefore N_2 t = N_o \frac{[\frac{KN_o t}{2}]^2}{\left(1 + \left[\frac{KN_o t}{2} \right] \right)^3} \quad (2.35)$$

For triple particles (m = 3)

$$\frac{N_3 t}{N_o} = \frac{[\frac{KN_o t}{2}]^3}{\left(1 + \left[\frac{KN_o t}{2} \right] \right)^4} \quad (2.36)$$

$$\therefore N_3 t = N_o \frac{[\frac{KN_o t}{2}]^3}{\left(1 + \left[\frac{KN_o t}{2} \right] \right)^4} \quad (2.37)$$

Finally, the evaluation of coag-flocculation efficiency or coag-flocculant performance of the process was obtained by applying the relation below.

$$E_{i_j}\ (\%) = \left(\frac{N_o - N_t}{N_o} \times 100 \right) \quad (2.38)$$

Materials and Method

Materials sampling, preparation and characterization.

Pharmaceutical Industry Effluent (PIE)

The effluent sample was collected from a local pharmaceutical industry situated in Anambra State, Nigeria. The characterization of the wastewater presented in table 1 was determined in line with standard procedure [35] ; [36] .

***Telfairia occidentalis* Seed Sample Collection**

Telfairia occidentalis Seed (TOS) sample. *Telfairia occidentalis* sample (precursor to TOSC) was sourced from Enugwu-Ukwu, while the aluminum sulphate (analytical grade) was sourced from head bridge market Onitsha, all in Anambra State, Nigeria. The TOS was processed according to the procedure reported by [13].

Characterisation of *Telfairia occidentalis* seed coagulant (TOSC)

100g of TOSC was characterized based on the procedure reported by [37] and presented in table 2.

Coag-flocculation Experiment

The Jar test was carried out based on standard Bench scale Nephelometric method. Appropriate dose of TOSC in the range of 0.1 – 0.7x10^{-3}kg/m^3 was added to 250ml of PIE. The suspension, tuned to PH range 1, 3, 5, 7, 10 and 13 by addition of 10M HCL/NAOH, subjected to 120secs. of rapid mixing (126 rpm) 1200secs of slow mixing (10rpm) using 688644A Gulenhamp magnetic stirrer followed by 2400secs. of settling. During settling samples were withdrawn from 2cm depth and changes in total dissolved and suspended solid (TDSS) measured for functional parameters using lab-Tech model 212R Tubidimeter at various time intervals of (2,4,6,10,20,30 and 40)x60secs. The same method was followed for the aluminum sulphate coagulant. The entire experiment was conducted at room temperate. The data generated were subsequently fitted in appropriate models for optimal functional parameters evaluation and comparative purposes.

Table 1: Characteristic of pharmaceutical industry effluent sample before treatment

Parameter	Values
Temperature (^{o}C)	28
Electrical conductivity (µs/cm)	4.9 x 10^2
pH	3.87
Phenol (mg/l)	Nil
Odor	acidic
Total hardness (mg/l)	6,000
Calcium (mg/l)	594
Magnesium (mg/l)	250
Chlorides (mg/l)	100
Dissolved oxygen (mg/l)	20
Biochemical oxygen Demand (mg/l)	50
Turbidity (mg/l)	1256
Iron (mg/l)	Nil
Nitrate (mg/l)	Nil
Total acidity (mg/l)	250
Total dissolved solids (mg/l)	225
Total suspended solids (mg/l)	57.25
Total viable count (cfu/ml)	9 x 10^1
Total coliform MPN/ 100ml	Nil
Total coliform count, cfu/ml	1 x 10^1
Faecal count MPN/mL	Nil
Clostridium perfrigens MPN/ml	Nil

Table 2: Characteristics of 100g of the seed kernel (TOSC precursor)

Parameter	Value
Moisture Content %	0.01
Crude Protein Content %	27.0
Crude Fibre %	3.0
Ash Content %	2.0
Fat & oil Content %	53.0
Carbohydrates Content %	15.0

Table 3: Coag-Flocculation Kinetic Parameters and Linear Regression Coefficient of TOSC at Varying Dosage and Optimal pH 13

Parameters	**$0.1x10^{-3}$ Kg/m^3**	**$0.2x10^{-3}$ Kg/m^3**	**$0.3x10^{-3}$ Kg/m^3**	**$0.4x10^{-3}$ Kg/m^3**	**$0.5x10^{-3}$ Kg/m^3**	**$0.6x10^{-3}$ Kg/m^3**	**$0.7x10^{-3}$ Kg/m^3**
α	2.000	2.000	2.000	2.000	2.000	2.000	2.000
R^2	0.660	0.659	0.699	0.752	0.827	0.675	0.674
K(m^3/kg.S)	7.5E-05	3.21E-05	7.701E-06	1.012E-05	3.50E-06	4.764E-06	4.46E-06
K_f (m^3/S)	1.5826E-19	1.5826E-19	1.5826E-19	1.5826E-19	1.5852E-19	1.5852E-19	1.5852E-19
$(a_{cf})_{BR}$ (m^3/kg.S)	1.5E-04	6.42E-05	1.542E-04	2.024E-05	7.0E-06	9.528E-06	8.92E-06
ε_p(kg $^{-1}$)	9.4781E+14	4.0566E+14	9.7435E+13	1.2789E+14	4.4158E+13	6.0106E+13	5.6271E+13
$\tau_{1/2}$(Sec)	12.88	30.10	125.46	95.47	276.05	202.81	216.63
(-r)	7.5E-05N_t^2	3.21E-05N_t^2	7.701-06N_t^2	1.012-05N_t^2	3.50E-06N_t^2	4.764E-06N_t^2	4.46E-06N_t^2
N_0(kg/m^3)	459.3477	744.6016	1080.7306	1336.7197	1192.6058	1502.855	1481.4815

Table 4: Coag-Flocculation Kinetic Parameters and Linear Regression Coefficient Alum at Varying Dosage and Optimal pH10

Parameters	**$0.1x10^{-3}$ Kg/m^3**	**$0.2x10^{-3}$ Kg/m^3**	**$0.3x10^{-3}$ Kg/m^3**	**$0.4x10^{-3}$ Kg/m^3**	**$0.5x10^{-3}$ Kg/m^3**	**$0.6x10^{-3}$ Kg/m^3**	**$0.7x10^{-3}$ Kg/m^3**
α	2.000	2.000	2.00	2.000	2.000	2.000	2.000
R^2	0.656	0.669	0.61	0.672	0.669	0.657	0.675
K(m^3/kg.S)	1. 34E-04	2.35E-05	8.078E-06	3.998E-06	5.95E-06	6.243E-06	6.20E-06
K_f(m^3/S)	1.5647E-19	1.5647E-19	1.5668E-19	1.5668E-19	1.5668E-19	1.5699E-19	1.5699E-19
$(a_{cf})_{BR}$(m^3/kg.S)	2.68E-04	4.7E-05	1.6156E-05	7.996E-06	1.19E-05	1.2486E-05	1.24E-05
ε_p(kg $^{-1}$)	**1.7128E+14**	**3.0038E+14**	**1.0311E+13**	**5.1034E+13**	**7.5951E+13**	**7.5951E+13**	**7.8986E+13**
$\tau_{1/2}$(Sec)	**8.11**	**46.25**	**134.56**	**271.88**	**182.68**	**174.11**	**175.32**
(-r)	**134E-04N_t^2**	**2.35E-05N_t^2**	**8.078-06N_t^2**	**3.998-06N_t^2**	**5.95E-06N_t^2**	**6.243E-06N_t^2**	**6.20E-06N_t^2**
N_0(kg/m^3)	**271.0762**	**481.6956**	**867.9802**	**1069.1757**	**1061.3458**	**750.2438**	**1416.4306**

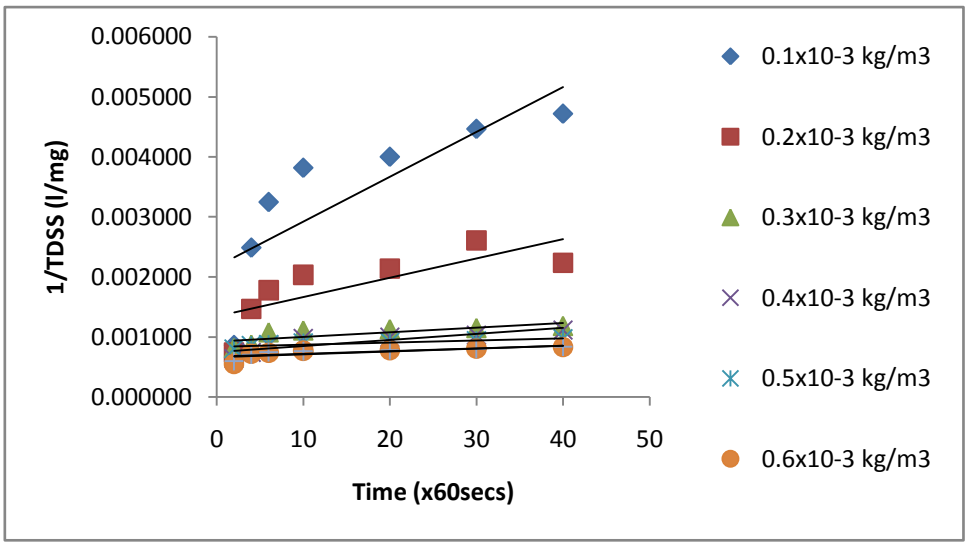

Figure 1a: Kinetic plot of TDSS removal using varying TOSC doses for PIE at pH 13

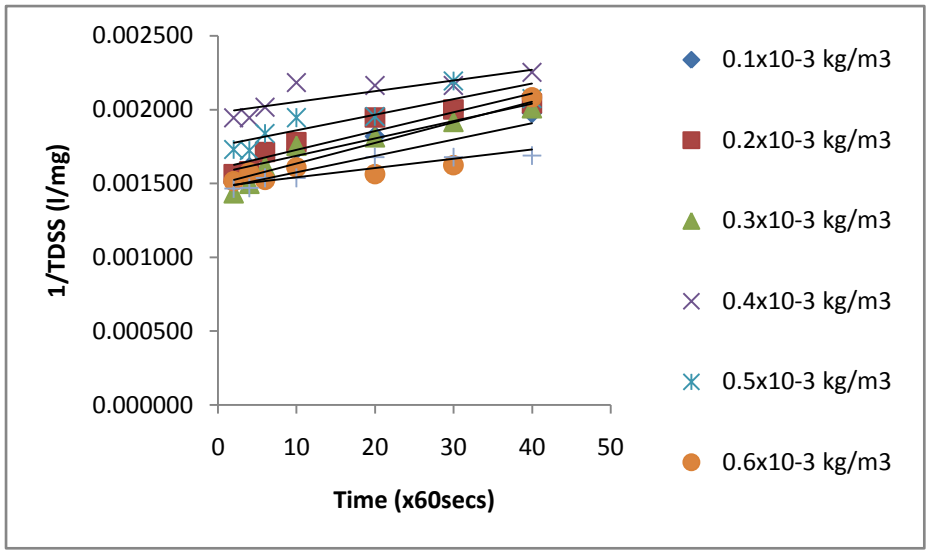

Figure 1b: Kinetic plot of TDSS removal using varying ALUM doses for PIE at pH 13

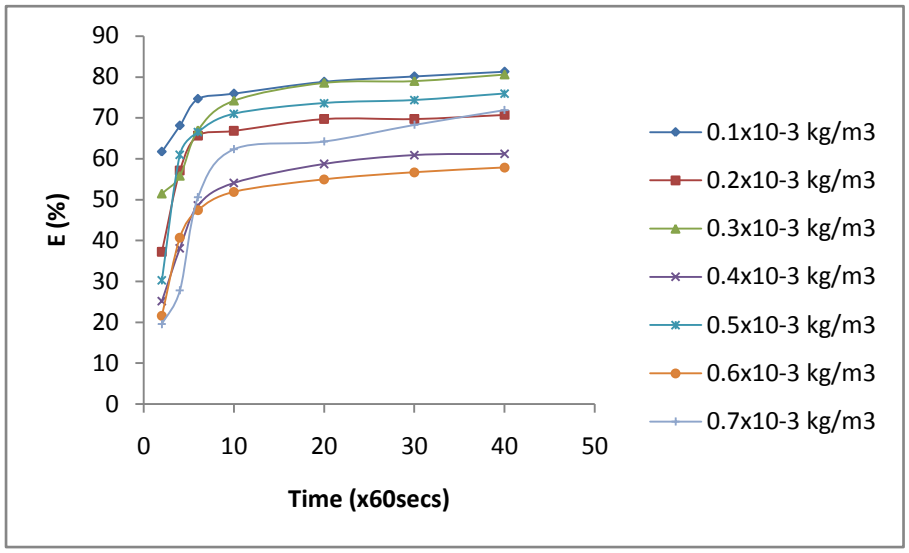

Figure 2a: Selected Efficiency(E%) plot of TDSS removal using varying TOSC doses for PIE at pH 10

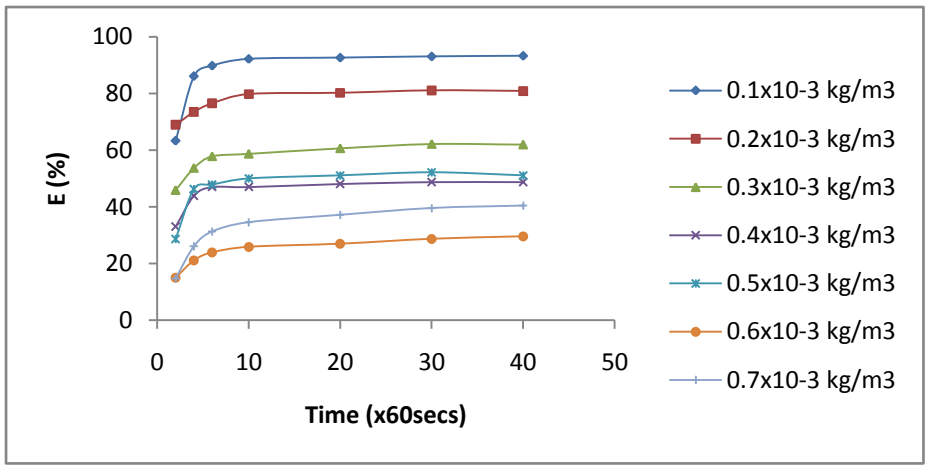

Figure 2b: Selected Efficiency(E%) plot of TDSS removal using varying ALUM doses for PIE at pH 10

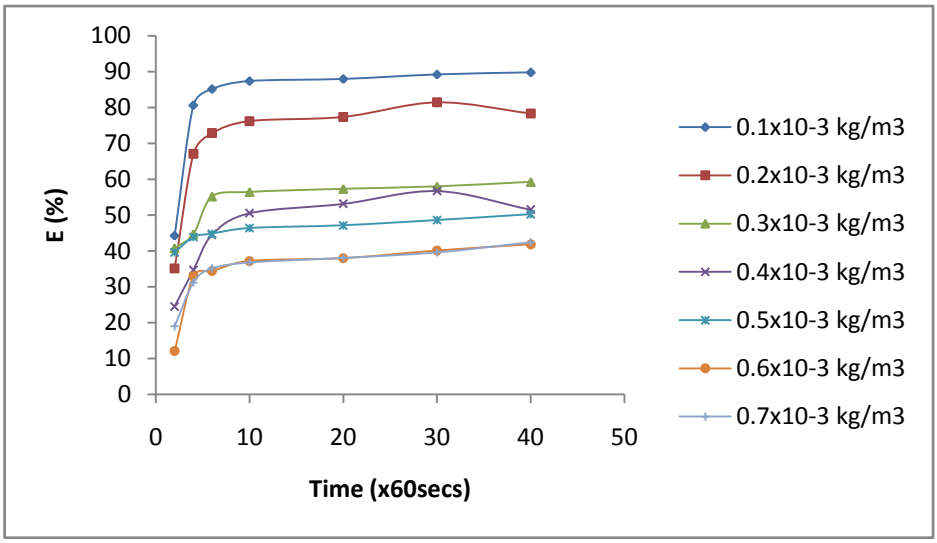

Figure 3a: Selected Efficiency(E%) plot of TDSS removal using varying TOSC doses for PIE at pH 13

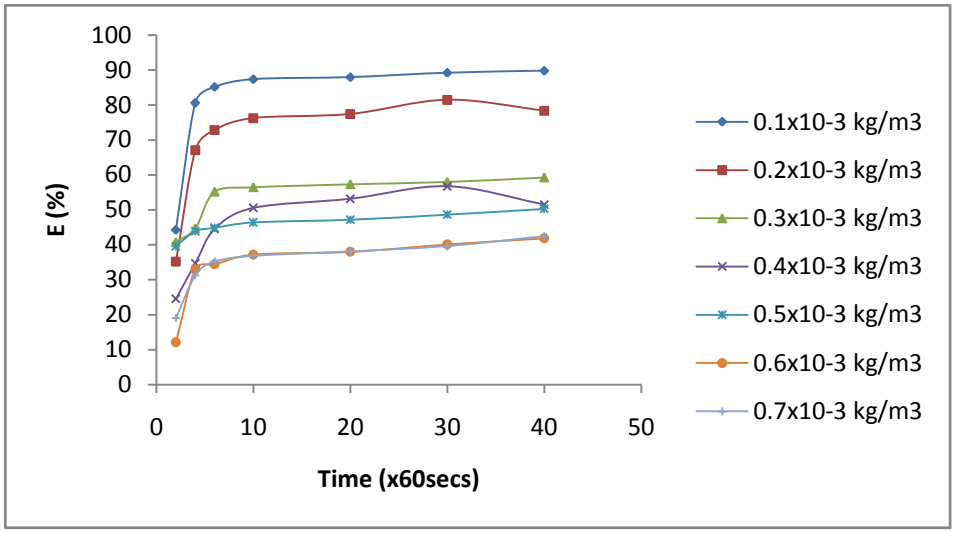

Figure 3b: Selected Efficiency(E%) plot of TDSS removal using varying ALUM doses for PIE at pH 13

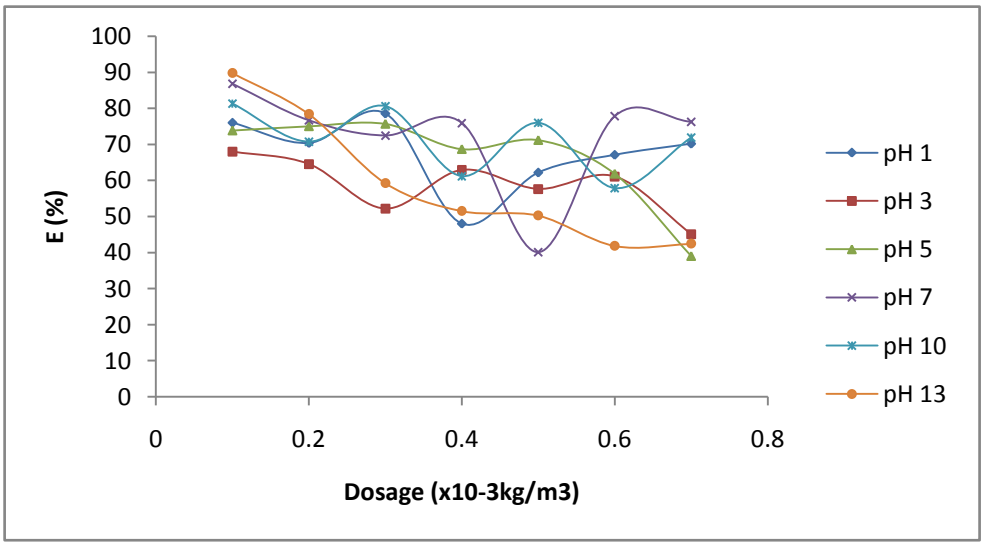

Figure 4: Efficiency(E%) plot of TDSS removal Vs TOSC Dosages at 40mins for varying pH

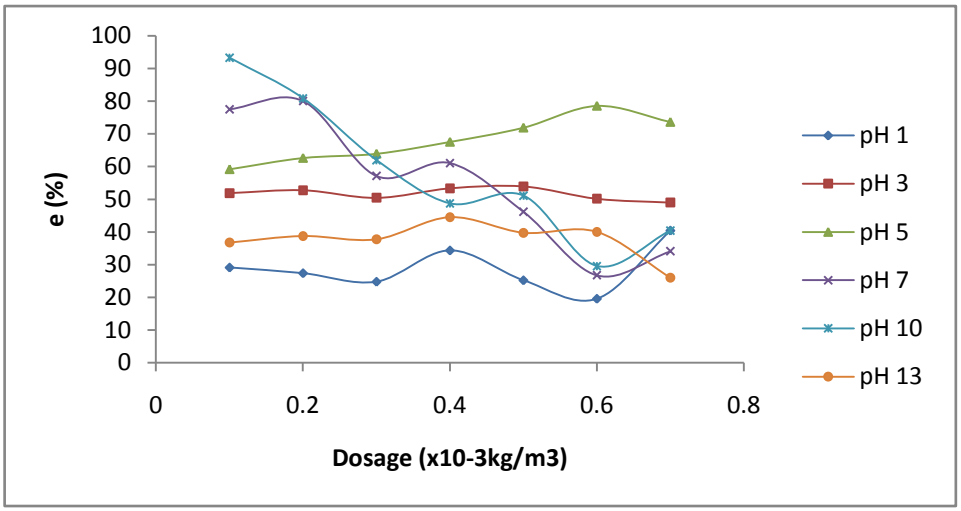

Figure 5: Efficiency(E%) plot of TDSS removal Vs ALUM Dosage at 40mins for varying pH

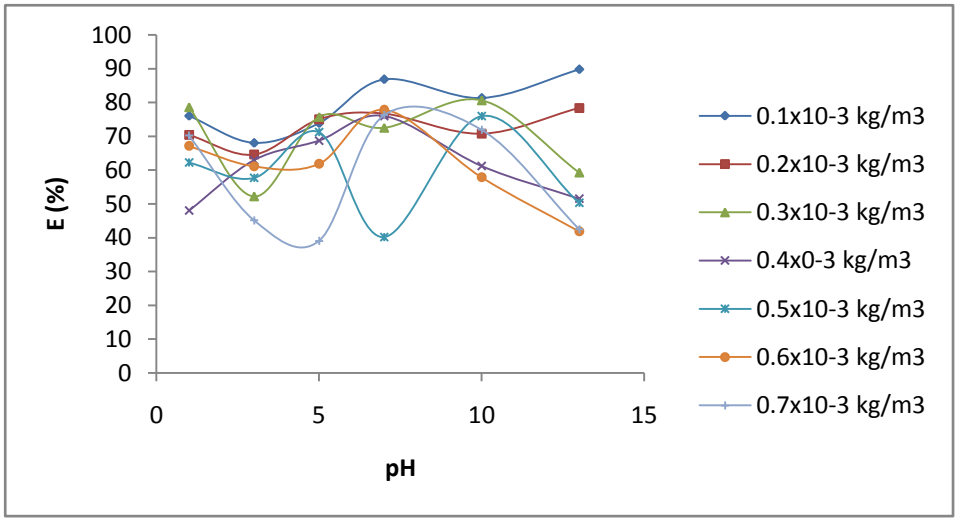

Figure 6: Efficiency(E%) plot of TDSS removal Vs pH at 40mins for varying TOSC dosages

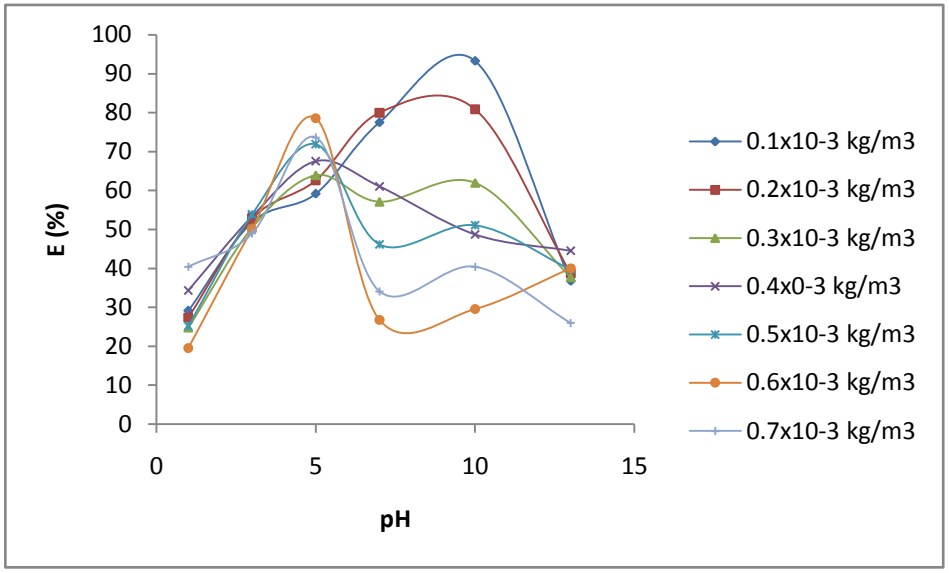

Figure 7: Efficiency(E%) plot of TDSS removal Vs pH at 40mins for varying ALUM dosages

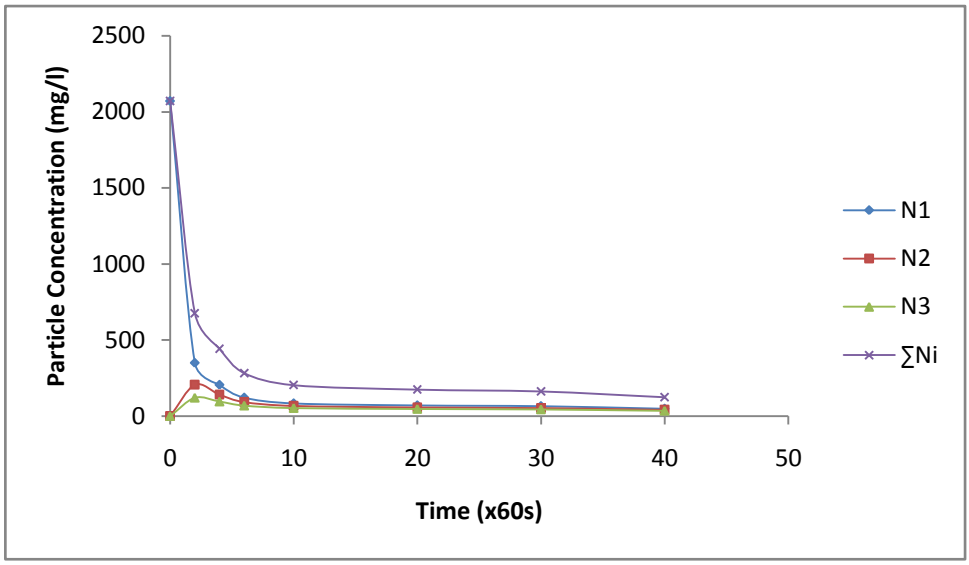

Figure 8a: Particle aggregation profile as a function of Time for minimum $\tau_{1/2}$ =12.88secs (TOSC)

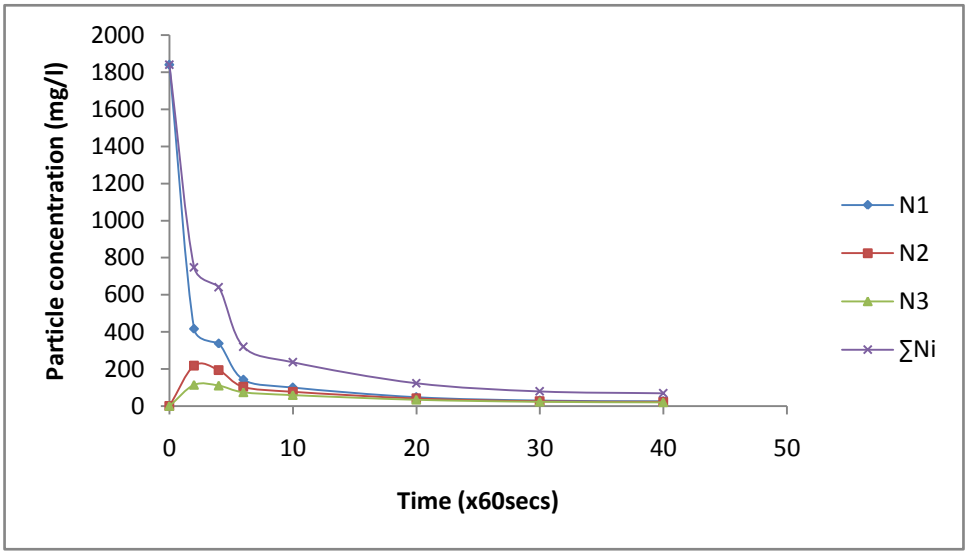

Figure 8b: Particle aggregation profile as a function of Time for minimum $\tau_{1/2}$ =8.11secs (ALUM)

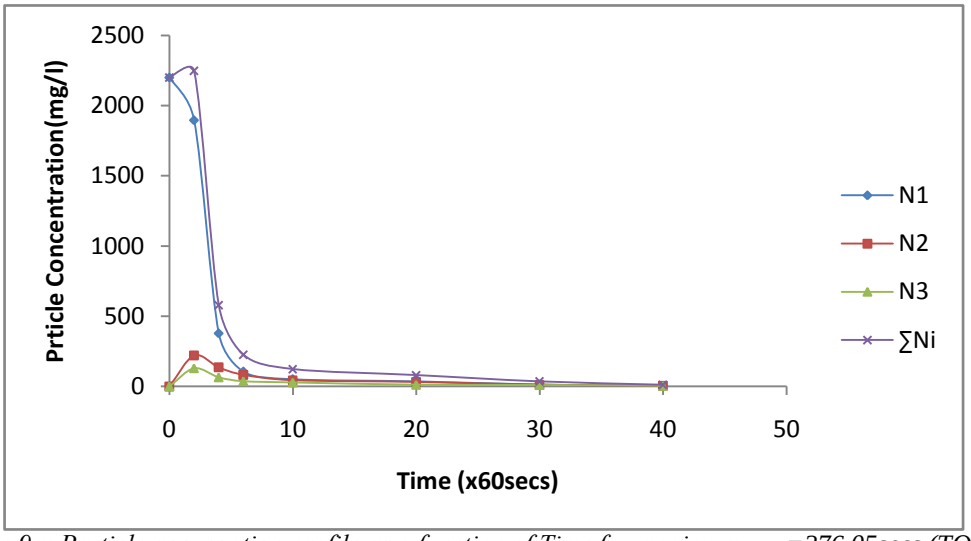

Figure 9a: Particle aggregation profile as a function of Time for maximum $\tau_{1/2}$ =276.05secs (TOSC)

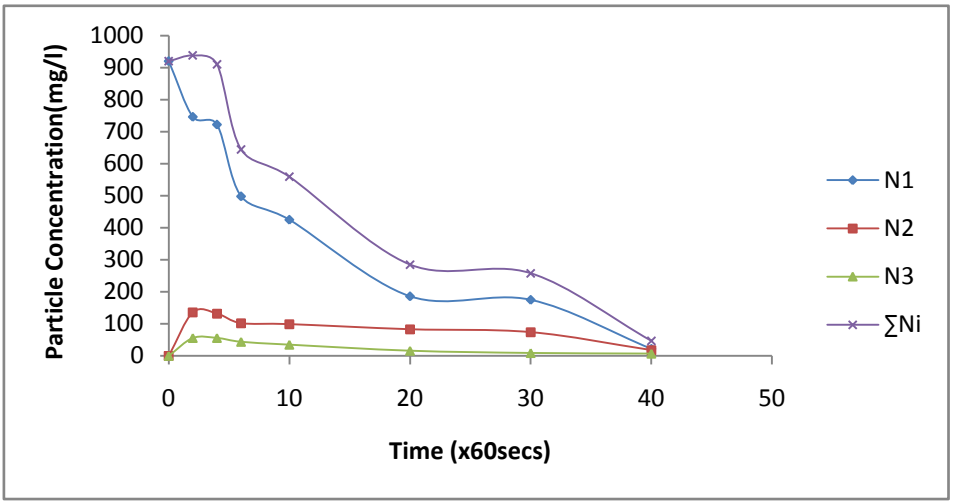

Figure 9b: Particle aggregation profile as a function of Time for maximum $\tau_{1/2}$ =271.88secs (ALUM)

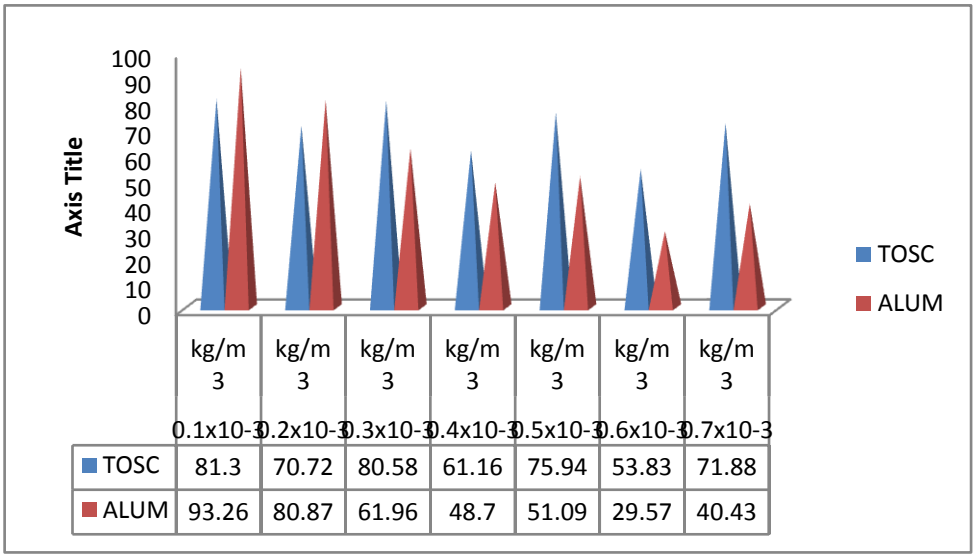

	kg/m3 0.1x10-3	kg/m3 0.2x10-3	kg/m3 0.3x10-3	kg/m3 0.4x10-3	kg/m3 0.5x10-3	kg/m3 0.6x10-3	kg/m3 0.7x10-3
TOSC	81.3	70.72	80.58	61.16	75.94	53.83	71.88
ALUM	93.26	80.87	61.96	48.7	51.09	29.57	40.43

Figure 10: Particle aggregation performance at 2400secs and pH 10 for varying TOSC and ALUM dosages

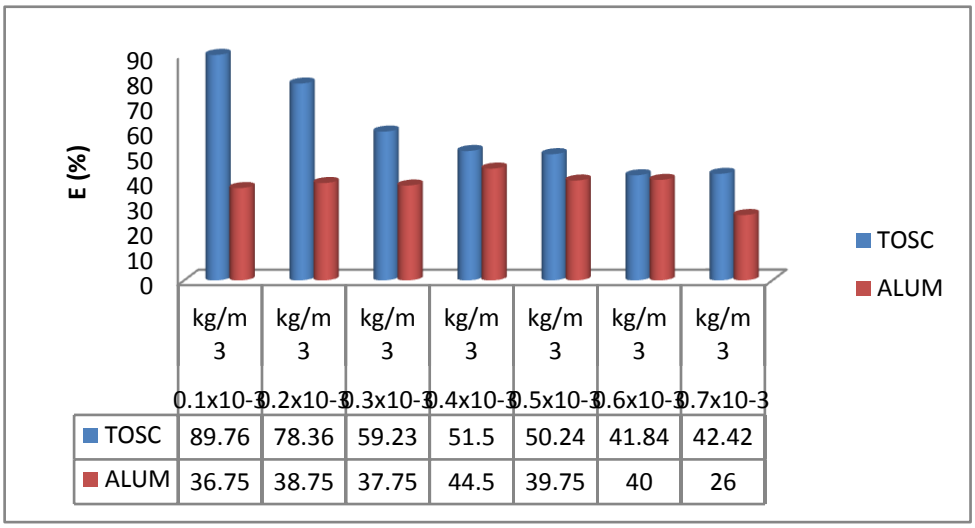

	kg/m3 0.1x10-3	kg/m3 0.2x10-3	kg/m3 0.3x10-3	kg/m3 0.4x10-3	kg/m3 0.5x10-3	kg/m3 0.6x10-3	kg/m3 0.7x10-3
TOSC	89.76	78.36	59.23	51.5	50.24	41.84	42.42
ALUM	36.75	38.75	37.75	44.5	39.75	40	26

Figure 11: Particle aggregation performance at 2400secs and pH 13 for varying TOSC and ALUM dosages

Results and Discussion

Characterization Results

The results obtained from the characterization of pharmaceutical industry effluent and *Telfairia occidentalis* seed were presented in tables 1 and 2. These are the major properties to be considered prior to choosing the appropriate treatment method in conjunction with the coagulant for the application of coag-flocculation treatment of PIE. Table 1, show that PIE has the following major characteristics, total dissolved solids, total suspended solids, Biochemical oxygen demand BOD, total viable count, total alkalinity (as calcium carbonate) and total acidity. These are the principal factors determining the level of turbidity in effluents. High level of these parameters result to high turbidity in the effluent, which prompted this study. The high alkalinity nature of the PIE translates to high TOSC dosage for TDSS removal as deduced from the experimental result. This is an indication that high alkalinity effluent will require higher coagulant dosage to reach the optimal conditions than that of lower alkalinity [38]. The pH value shows that the PIE is relatively strongly acidic and this affected the odor. The acidic nature of the PIE increases its conductivity value to a level which apparently implies that the sludge sample after treatment contains ionic radicals, providing conditions for the choice of treatment method employed. Also the value of total dissolved solids is relatively high indicating formation of high volume of solid sludge with incorporation of some essential minerals and devoid of metals, making it suitable as soil nutrients for agricultural purposes and in landfills. However, the acidic nature of the PIE might be responsible for the low non-ionic bacteriology parameters load obtained, because some organisms may not exist in high acidic medium.

Meanwhile, table 2, show that 100g of the seed kernel (TOSC- precursor) has relatively high crude protein content, fats and oil respectively. This is indication that TOSC with the presence of a water-soluble cationic crude protein (inherently with amine groups) can suitable be applied for PIE treatment. However, the presence of oil along with many other organic compounds in it increases organic matter content of the treated effluent, which is in line with previous similar work [39] .

Coag-flocculaion Activities

A summary of the coag-flocculation kinetics parameters of TOSC and Alum at their optimum conditions as determined in this study are shown in tables 3 – 4 for varying dosages. The reliability of the experimental data obtained were ascertained by fitting them into the generalized model equation 2.26, providing condition for the evaluation of squared linear regression coefficient (R^2). Table 3 – 4 indicates that experimental, data with $R^2 >$ 65 is apparently described by the linearised form of Equation 2.25 at the early stage of coag-floculation and optimum pH conditions for TOSC, Alum respectively. K is determined from the slope of equation 2.26 demonstrated in figures 1a and 1b (Kinetic plot of $1/N_t$ Vs time).

The results presented in tables 3 – 4 show that K and $(a_{cf})_{BR}$ has minimal variations with dosage variation especially for 0.2, 0.4, 0.5, 0.6 and $0.7x10^{-3}kg/m^3$-TOSC and 0.1 – $0.4x10^{-3}kg/m^3$ – Alum respectively. This could be as a result of equal amount of TDSS sorption rate on the coagulants interface achieved by those dosages depicted in figures 2 and 3. However K is related to $(a_{cf})_{BR,}$ from the expression designated as equation 2.16 ($2K = (a_{cf})_{BR}$), which implies that alternatively K can be evaluated from equation 2.16. It could be observed from tables 3 and 4, that the optimum conditions are recorded at pH 13, $0.1x10^{-3}kg/m^3$ TOSC and pH 10, $0.1x10^{-3}kg/m^3$ Alum respectively. Also from the tables 3 and 4, show that the best performance were achieved at the alkaline region, for both coagulants though at different magnitude. The implication is that application of coag-flocculation techniques of PIE treatment using TOSC and Alum coagulants are better in alkaline medium, following easy hydrolysable in the effluent to form cationic complexes for TDSS attachments, though not at the same rate. This phenomenon is supported by different optimal K values obtained for the coagulants: Alum – 1.34E – 04 m^3/ kg.s, pH 10; TOSC – 7.5 x E – 05 m^3/kg.s, pH 13 at $0.1x10^{-3}kg/m^3$ each). The high rate obtained for $0.1x10^{-3}kg/m^3$ at the condition of this study amplified the fact that there is zeta potential at the boundary of the hydrodynamic shear plane of charged particles in PIE alkaline medium. This implies that low zeta potential values provide greater instability (by way of degreasing electrostatic repulsion between charged surfaces). It is understandable that at this point the negative charge of Zeta potential has been interchanged with the positive charge from the coagulants to form zeta potential cation (PZC). At this point, the TDSS particles possess the lowest stability, providing condition for maximum aggregation or sorption on the coagulants interface.

The values of $\tau_{1/2}$ obtained from equation 2.31 and evaluated for TOSC and Alum at $0.1x10^{-3}kg/m^3$doses respectively $\tau_{1/2}$ = 12.88secs- TOSC and $\tau_{1/2}$ =8.11secs – Alum, supports the optimal values of K recorded at $0.1x10^{-3}kg/m^3$ for both. The period of 12.88secs and 8.11secs are the lowest recorded for TOSC and Alum respectively, and indication of best performances at the same dosage and different pH. The optimal $\tau_{1/2}$ values recorded for the coagulants at the same dosage and different pH are satisfactory, though milliseconds has been reported in previous works [32] . It is observed from equation 2.31 that $\tau_{1/2}$ is dependent on the initial concentration $N_{o,}$ hence high N_o is a condition for lower $\tau_{1/2}$. This accounts for high clarification rate achieved in this work with high initial TDSS loads 2070 mg/l and 1840mg/l for the various pH under consideration. ε_p and

k_f were obtained from equations 2.7 and 2.8 respectively. On substitution of equation 2.8 into 2.7 yields ε_p. Tables 3- 4, indicate insignificant variations in the $K_f = f(T, \eta)$ values obtained, due to negligible changes in the values of temperature and viscosity of the PIE medium. At near constant value of K_f, ε_p relates proportionally to $2K = (a_{cf})_{BR}$ expressed as equation 2.17. Thus high ε_p results in high kinetic energy to overcome the zeta potential existing at the boundary of the hydrodynamic shear plane (i.e between the charged particles and effluent medium). From the aforementioned, it can be deduced that $\tau_{1/2}$, ε_p and k_f are the effectiveness factors responsible for the coagulation performance before flocculation sets in. The values of (–r) or (dN_t/dt) is evaluated from equation 2.6 and posted in tables 3 and 4. The expression in equation 2.6 indicate that (–r) or $(dN_t/dt) = f(K, N^{\alpha}_t)$, which implies that rate of TDSS depletion or removal is mainly dependent on the coagulation rate constant K and level of TDSS present in the effluent medium. Thus, high K value is a condition for maximum TDSS removal efficiency by the coagulants as can be seen from the tables 3-4

The discrepancies observed in some functional parameters values posted in tables 3 and 4 from the norms could be adduced to the following: inadequacies in mixing parameters (slow and rapid), including time and intensity of mixing. Ample time should be given for slow and rapid mixing in order to achieve maximum TDSS removal efficiency because coagulation process is known to be time dependent and other factors. The implication is that the time given for slow and rapid mixing in this work may not be adequate. Another factor is the hydrodynamic interactions arising from mechanical agitation of the suspension plays an important role in TDSS removal efficiency. Vigorous agitation of the suspension causes floc breakage and exposure of fresh surfaces to TDSS sorption, thereby increasing adsorption capacity. But the rate of adsorption is not proportional to increased floc breakage.

Plot Of TDSS removal efficiency vs time

This actually depicts how TDSS removal efficiency varies with time. The removal efficiency is obtained based on evaluation of equation 2.38. The graphical results represented in figures 2a, 2b – 3a, 3b are obtained for the optimal pH of TOSC and Alum. Figures 2a, 2b – 3a, 3b are obtained for the optimal pH of TOSC and Alum. The figures, indicate that $0.1x10^{-3}kg/m^3$ doses of TOSC and Alum were found to be most effective in removing TDSS for pH and settling time of 13, 10 and 2400secs each respectively. The best performance recorded at $0.1x10^{-3}kg/m^3$ for both were amplified with the initial TDSS load of 2070 mg/l – TOSC and 1840 mg/l Alum reduced to 211.97 mg/l indicating that equivalent of 89.76% TDSS efficiency is achieved, whereas that of alum is reduced to 124.02 mg/l (93.26%), all taken place at the end of 2400secs. It can be deduced from the figures 2a, 2b – 3a, 3b that increase in doses at the experimental conditions does not affect the effective performances of the coagulants (TOSC and Alum). The results show that both coagulants had similar effects despite different species and pH involved. This impressive performance by TOSC at lower dosage beyond $0.1x10^{-3}kg/m^3$ will result in a higher number of amino groups, causing entanglements between polymer chains themselves due to interaction among amino and hydroxyl – methyl groups on TOSC chains thereby reducing the number of active amino groups for coagulation with TDSS particles. Whereas the effectiveness of alum at $0.1x10^{-3}kg/m^3$ dosage is because of its ability to readily form multi-charged/poly -nuclear complexes with enhanced adsorption characteristics, though the nature of complexes formed may be controlled by the pH of the effluent. With these remarkable performances observed, these systems (PIE – TOSC and PIE – Alum) had shown features of systems characterized by high cationic charge on the coag-flocculant and anionic TDSS which is obtainable at low coagulant dosage. This is an indication that the systems are controlled by electrostatic patch mechanism.

Plot of TDSS removal efficiency Vs dosage

This is evaluated from equation 2.38 and demonstrated in figures 4 – 5. The figures actually confirms the extent to which the coagulants doses of TOSC and Alum respectively affected the TDSS removal efficiency at the existing optimal pH values. The significant features observed in the systems is that coagulant dosage increase does not influence the effectiveness of the coagulants studied as can be ascertained from figures 4 – 5. However, the optimum dosage of $0.1x10^{-3}kg/m^3$ is observed to achieve the highest TDSS removal efficiency of 89.76% and 93.26% for TOSC and Alum respectively. Beyond this value, the rate of TDSS removal decreases. This is contrast to the fact that with more doses of TOSC and alum, more charged sites are available for uptake of colloidal particles (in form of TDSS) from the PIE. This could be that increased doses of these coagulants beyond a certain level may favor competitive TOSC – TOSC; alum-alum associations at the expense of TOSC – TDSS, Alum – TDSS, particle interaction respectively. It might also lead to counter ion re-stabilization causing the dispersion of the flocs and subsequently affecting the settling of the particles which is in line with previous similar work [40] .

Plot of TDSS removal efficiency Vs pH.

The effect of pH on TDSS removal efficiency at the varying coagulants dosages is investigated. The efficiency values evaluated from equation 2.38 x-rayed how TDSS removal is affected by the pH of the effluent medium at the end of 2400secs settling time, presented in figures 6–7. The figures show that TDSS removal increased with

increasing pH up to 13 and 10 for TOSC and Alum, respectively. When pH increased from 1-13, TDSS removal efficiency increased from 76 – 89.76% for TOSC, whereas for Alum, the pH increased from 1 – 10, TDSS removal efficiency increased from 29.13 – 93.26% at $0.1x10^{-3}kg/m^3$ dosage each, beyond this point the value drastically decreased. It can be seen in figure 7, that high acidic and high alkaline pH for alum caused lower efficiency. However, alum is effective at pH 10. Whereas in figure 6, high acidic and high alkaline pH for TOSC did not have much effect on the efficiency because the values obtained at both acidic and alkaline regions were satisfactory at the dosage under consideration. However, TOSC is effective at pH 13. The major difference between figure 6 and 7 is that from pH of 7 – 13 for $0.1x10^{-3}kg/m^3$, TOSC performance is better than the ones obtained from $0.2 – 0.7x10^{-3}kg/m^3$ under the same condition.

Time evolution of the cluster size distribution

On evaluation of equations 2.33 – 2.37, the time evolution of particle aggregates (singlets, doublets, triplets for m = 1, 2, 3, respectively) is predicted. The typical nature of the particles aggregation behavior in 12.88secs, 276.05secs, 8.11secs, 271.88secs for TOSC and alum respectively are presented in figures 8a, 8b – 9a, 9b. In figures 8a and 8b, the primary particles N_1 and total number of particles ΣN_i fused into one particle kernel at t =0; N_t= 2070 and 1840 mg/l to N_t = 676 and 748 mg/l for TOSC and Alum respectively (0 – 120secs). This is an evidence of either the existence of low shear resistance between the N_1 and ΣN_i at that point leading to TDSS particle entrapment or that the cationic charges of the coagulants overwhelms the anionic charges of the TDSS particles in PIE. Also the pairs of ΣN_i and N_1 can be seen to decrease more rapidly. This is case of high rate of coag-flocculation activity demonstrated at low $\tau_{1/2}$ of 12.88secs and 8.11secs for TOSC and alum respectively. Figures 8a and 8b indicate that the pairs of N_2 and N_3 are present at t = 0, N = 0 with low zeta potential between the particles.

Critical observation on figures 8a and 8b show that there are close interactions between the particles of N_1, N_2 and N_3 resulting to the formation of flocs as from 600secs to infinity and 1080secs to infinity for TOSC and alum respectively. The mechanism that accounts for the behavior are charge neutralization and floc sweep [28]; [20]. There is a small void in between N_1, N_2 and N_3 and ΣN_i from 120secs indicating a small margin of difference existing in the concentration of TDSS amongst them. The implication is the existence of low potential hump and resistance to aggregation. In figure 9a, the maximum aggregation of the sum of particles reached the maxima at 120secs. The sum of the particles can be seen to decrease more rapidly than the rest, indicating a moderately hyper slope at early stage of coag-flocculation activity. At t = o, both pairs of particles (i.e. ΣN_i, N_1, N_2 and N_3) had temporary collision though at different magnitude. The curves of N_2 and N_3 indicate that the highest particle cluster recorded at 120secs, suggesting that the system witnessed rapid coagulation at the early stage. Also the particles N_1, N_2 and N_3 started forming larger flocs at end of 600secs of the coag-flocculation process and subsequently the sum of particles ΣN_i joined after 1920secs ready to be sweep away following gravitational principles. Whereas figure 9b show curves that depicts presence of relatively high zeta potential in them, causing less attraction of TDSS particles in PIE with the coagulants cat ions except at t = 0 and 2400secs. This is an indication of a system being controlled by repulsive and shear force mechanisms.

Comparative Analysis of Coag-flocculation activities of TOSC and Alum

The coag-flocculation performance of TOSC and Alum was compared at their optimal pH (10 and 13) as presented in figures 10 and 11 respectively. The figures depicts the effectiveness of these coagulants in removing TDSS from PIE. The results obtained indicate that TOSC performed better than alum at the prevailing pH and dosages, with the exception of 0.1 and $0.2x10^{-3}kg/m^3$ for pH 10 where alum performed better than TOSC. However, the fact is that the performance of TOSC compares favorably with alum at its best at the same experimental condition. The impressive performance displayed by TOSC could be as result of the presence of complex positive amine species. This usually neutralizes TDSS charges including the zeta potential, leading to effectively lowering or removing the electrostatic energy barrier, hindering the intending coag-flocculating particles. With this occurrence the TOSC instantly sweeps away the TDSS [13] . The main advantage of TOSC over alum, is the achievement of impressive performance over a wide range of pH and dosages. Above all, its low production of sludge (biodegradable) post usage makes it environment friendly.

Conclusion

The application of TOSC as an effective coag-flocculation in removing TDSS from high turbid PIE over a wide range of pH and dosages has been established. The TDSS removal efficiency >89% of its initial value at the maximum coag-flocculation activity justifies its effectiveness with high rate constant and low coagulation period. The system can operate optimally at pH 13, $0.1x10^{-3}kg/m^3$ dosage and 2400secs settling time. The results obtained is in line with previous similar works [41] ;[20] .

NOMENCLATURE

K: αth order coag-flocculation constant

$(a_{cf})_{BR}$: Collision factor for Brownian Transport
ε_p: Collision Efficiency
$\tau_{1/2}$: Coagulation period/half life
E_{ij}: Coag-flocculation Efficiency for i and j particles.
R^2: Coefficient of Determination
α: Coag-flocculation reaction order
-r: Coag-flocculation mass transfer rate
TOSC: *Telfairia occidentalis* Seed Coagulant
TDSS: Total dissolved and suspended solids.
K_f : Rate Constant for rapid Flocculation

References

1. Mayabhate, S.P., Gupta, S.K., Joshi, S.G (1988). Biological treatment of pharmaceutical Wastewater. Water Air Soil. Poll., 38, 189 – 197.
2. Ravi Kumar, M.N.V., Sridhari, T.R., Bhavani, K.D., Dutta, P.K (1998). Trends in colour removal from textile mill effluents, colorage, 40, 25 – 34.
3. Ghebremichael, A.K (2004). Moringa Seed and pumice as alternative natural materials for drinking water treatment TRITA LWR PHD 1013 Ph.D. Thesis. KTH land and Water Resources Engineering.
4. Gupta, S.K, Gupta, S.K (2006). Treatment of pharmaceutical wastes, Indian Institute of Technology, Bombay, India, 167 – 233
5. Roth, V., Dong, Z., Senn, D., Maclead M., Shine, J (2005). Transport and Fate of selected priority pharmaceuticals in U.S. Harvard University, Boston, Management USA, Swiss Federal Institute of Technology, Zurich, Switzer land(ROT – 117 – 844293)
6. Benotti and Etho (2008). pharmaceutical as tracers of municipal wastewaters in urban Estuaries, (BEN – 117 – 831465)
7. Anderson, D.R. (1980). pharmaceutical wastewater treatment. A case study proceedings of 35th Industrial waste conference, purdue University, West Lafayette, In, 456-462.
8. Heberer, T.H, Stan, H.J (1997). Determination of Clofibric acid and N – (phenylsulfonyl) – Sarcosine in sewage, river and drinking Water, Int J. Environ Anal. Chem., 67,113.
9. Buser, H.R., Muller, M.D., Theobald, N (1998a). Occurrence of pharmaceutical drug clofibric acid and the herbicide meco prop in various Swiss lakes and in the North Sea. Environ Sci. Technol., 32(1) : 188
10. Buser, H.R., poiger, T., Muller, M.D (1999). Occurrence and environmental behavior of the Chiral pharmaceutical drug Ibuprofen in surface waters and in wastewater. Environ. Sci. Technol., 33 (15), 2529.
11. Buser, H.R., Poiger, T., Muller, M.D (1998b). Occurrence and fate of the pharmaceutical drug diclofenac in surface waters: rapid photodegradation in a lake. Environ. Sci. Technol., 32 (22): 3449
12. Kolpin, D.W., Furlong, E.T., Meyer, M.T., Thurman, E.M., Zaugg, S.D., Barber, L.B., Buxton, H.T (2002). Pharmaceuticals, hormones, and other organic wastewater contaminates in US streams, a national reconnaissance. Environ. Sci. Technol., 36 (6): 1202.
13. Ugonabo, V.I., Menkiti, M.C., Onukwuli, O.D (2012) Effect of coag-flocculation kinetics on *Telfairia occidentalis* seed coagulant (TOC) in pharmaceutical wastewater. International journal of Multidisciplinary Sciences and Engineering, 3,(9), 22-33.
14. McChang, S.M and Lemley, A.T (1994). Electrochemical treatment and HPLC Analysis of wastewater containing acid dyes. Text chem. color, 26, 17 – 22.
15. O' Neill, C., Hawkes, F.R., Hawkes, D.L., Esteves, S., Wilcox, S.J (2000). Anaerobic – aerobic biotreatment of simulated textile effluent containing varied ratios of starch azo dye. Wat. Res., 24, 2355 – 2361.
16. Yu-li, Y.R and Thomas, A (1995). Color difference measurement and color removing from dye wastewaters using different adsorbents. J. Chem. Tech. Biotechnol., 65, 55 – 59.
17. Sarasa, J., Rochie, M.P., Ormad, M.P, Gimeno, E., Puig, A., Overllerio, J.L (1997). Treatment of a wastewater resulting from dyes manufacturing with ozone and chemical coagulation Wat. Res., 32, 2721 – 2727.
18. Papic, S., Koprivance, N. Loncar,ic, B.A (2000). Removal of reactive dyes from wastewater using Fe(iii) coagulant. J. Soc. Dyers Color, 116, 352 – 358
19. Ugonabo, V.I., Menkiti, M.C., Atuanya, C.U., Onukwuli, O.D (2013). Comparative studies on coag-flocculation kinetics of pharmaceutical industry Effluent by Achatina Maginata Shell Biomass and

Aluminum Sulphate .International Journal of Engineering & Technology, IJET – IJENS, 13 (02), 134 – 147.
20. Menkiti, M.C., Aneke, M.C., Ogbuene, E.B., Onukwuli, O.D., Ekumankama, E.O (2012). Optimal Evaluation of coag-flocculation factors for Alum-Brewery Effluent system by Response surface methodology. Journal of minerals materials characterization & Engineering, 11 (5), 543 -558.
21. WU, X., Ge, X., Wang, D., Tang, H (2007). Distinct Coagulation Mechanism and model between alum and high Al13 – PACL colloids and surfaces A: Physiocochem. Eng. Aspects, ELSEVIER, 305, 89 – 96
22. Dentel, S. K and Gosset, J.M (1988). Mechanisms of coagulation with aluminum salts, J. AM. Water works Assoc., 88, 187 – 198
23. Duan, J and Gregory, J (2003). Coagulation by hydrolyzing metal salts. Adv. Colloid interface sci. 100 – 102, 475 – 502
24. Rose, G.R. and St. John, M.R (1987). Flocculation in Encyclopedia of polymer science and Engineering (H.F. Mark, N.M Bikales, C.G. Overberger, George Menges and J.I Kroschwitz, eds.) john Wiley & sons, New York, 7, 211
25. Gregory, J (1987). Flocculation by polymers and polyelectrolytes, in solid – liquid dispersions (Th. F. Tadros, ed) Academic Press (London) Ltd., Ch. 8.
26. Dorea, C.C (2010). Coagulant-based emergency water treatment, Desalination, 251, 83 – 90 (ELSEVER).
27. Twort, A.C., Ratnayaka, D.D., Brandt, M.J (2000). Water supply, 5th Ed. Amold publishers, London, UK.
28. Ugonabo, V.I., Menkiti, M.C., Onukwuli, O.D., Igbokwe, P.K (2013). Kinetics and functional parameters Response of Aluminum sulphate coagulant to variation in coag-flocculation variable in High turbid pharmaceutical industry Effluent. International Journal of Engineering and Innovative Technology (IJEIT), 2 (9), 25 – 35.
29. Feuillebois, F. J (1989). Colloid inferface sci, 131:267
30. Merrtt, R.M and Subramanian, R.S (1989). J. Colloid Interface Sci., 131:514
31. Barton, K.D. and Subramanian, R.S (1989). J. Colloid interface sci., 133:214
32. Von smoluchowski, M (1917).Z. Phys chem., 92:129
33. Zhang and Davis, R.H (1991). Journal of fluid mech., 230:479
34. Wang, H and Davis, R.H (1993). Journal of colloid interface sci., 159:108.
35. WST (2005). About Coagulation and Flocculation: Information Bulletin, U.S.A.
36. AWWA (2005). American Water works association standard methods for the examination water and wastewater effluent, New York, USA.
37. Rezig, L., Chouaibi, M., Msaada, K., Hamdi, S (2012). Chemical composition and profile characterization of pumpkin (Cucurbita Maxima) seed oil. Journal of industrial crops and products. Science of the total Environment, 37, 82 – 87
38. White, M.C., Thompson, J.D., Harrington, G.W., Singer, P.C (1997). Evaluating criteria for enhanced coagulation compliance. J.AM Water Works Ass., 89, 64 – 77.
39. Ndabigengesere, A., Narasiah, K.S (1988). Quality of water treated by coagulation using Moringa Oleifera seeds. Water Research, 32, 781 – 791
40. Stephenson, R.J., Duff, S.J.B (1996). Coagulation and precipitation of a mechanical pulping effluent .1. Removal of carbon, color and turbidity. Wat Res., 30 (4), 781 – 792.
41. Lin, D.Q., Brixius, P.J, Hubbuch, J.J, Thompson, J., Kula, M.R (2003). Biomass/adsorbent electrostatic interactions in expanded bed Bioengineering, 83 (2), 149 – 157.